Paper No.
5588

NACE INTERNATIONAL CORROSION 2015 CONFERENCE & EXPO

Corrosion Behavior of Buried Pipeline in Presence of AC Stray Current in Controlled Environment

Elmira Ghanbari
National Center for Education and Research on Corrosion and Materials Performance, Department of Chemical and Biomolecular Engineering, University of Akron
302 E Buchtel Ave
Akron, OH 44325
USA

Scott Lillard
National Center for Education and Research on Corrosion and Materials Performance, Department of Chemical and Biomolecular Engineering, University of Akron
302 E Buchtel Ave
Akron, OH 44325
USA

Mariano Iannuzzi
General Electric Oil & Gas
Eyvind Lyches vei 10
Sandvika, 1338
Norway

Mauricio Rincon Ortiz
Universidad Industrial de Santander
Cr 27 calle 9
Bucaramanga, Santander, 680002
Colombia

ABSTRACT

Alternate current (AC) corrosion is a frequent problem where pipelines share right of way with high power transmission lines, AC powered railed system, and structural components on subsea power units. The magnetic field produced by transmission power lines and AC power generators and converters induces an alternate electric current on the buried pipe; the magnitude of the induced AC being proportional to the voltage and separation distance. It has been reported that AC corrosion can occur even when the cathodic protection (CP) criteria is satisfied, highlighting the fact that AC interactions are not well understood. In the present work, corrosion rates of carbon steel samples in sodium chloride solutions with and without AC at different DC bias potentials were obtained by both electrochemical techniques and weight loss analysis. Results are compared and discussed together with polarization curves to obtain an assessment of electrochemical techniques, which are commonly applied for evaluation of AC induced corrosion. A correlation between corrosion rates obtained from weight loss and electrochemical techniques was obtained by comparing corrosion current densities estimated from weight loss values with those from polarization curves. These results are discussed in the context of differences in the anodic and cathodic Tafel slopes. Additionally, solution analyses were conducted during the test to quantify the ferrous/ferric ion content and solution pH. Stirring and continuous solution replacement were necessary to maintain a constant ferrous/ferric ion content and pH.

Key words: AC interference, corrosion, carbon steel, kinetic parameters, Tafel slopes

INTRODUCTION

Background

AC induced corrosion has been known to occur for quite some time, as long as 100 years ago the NIST[(1)] issued a technical paper on the “Influence of Frequency of Alternating or Infrequently Reversed Current on Electrolytic Corrosion”.[1] However, it was not until an accident on a pipeline in Germany in 1986 that it became a widespread industrial topic and safety concern. The failure occurred on a polyethylene coated pipe installed in 1980 parallel to a 16.6 Hz powered railway. The pipeline was cathodically protected at –1000 mV vs. SCE, typical of European industry standards of the time. The failure surface was described as having crater-like corrosion pits below corrosion product that resembled "bulges”.[2] It was concluded that a low soil resistivity of 1900 ohm-cm from de-icing salts was a contributing factor in the failure. Since then there have been numerous field cases of AC induced failures in systems with otherwise adequate CP with rapid penetration rates and tubercle formation being common phenomena. As a result, both international and US standards as well as "best practices" have been published detailing corrosion protection criteria to mitigate AC-induced corrosion.[3,4] Since the failure in Germany there has also been a large number of laboratory studies focused on characterizing the variables that contribute to AC induced corrosion. Of particular importance are, AC pipe-potential (or AC pipe current), level of cathodic protection and the spread resistance.

AC Mitigation and CP Criteria

It is generally agreed that at the open circuit potential (OCP), increasing the AC pipe-potential and, correspondingly, the AC-pipe current results in an increase in corrosion rate. While some protection is obtained using a CP potential criterion of -0.85 V vs. SCE, it is not until the CP potential is reduced to -1.0 V vs. SCE that the effects of AC can be completely mitigated.[5] For most AC pipe-currents, protection can be achieved using CP currents between 0.1 A/m^2 and 20 A/m^2.If the CP current is too high, however, a region of high corrosion has been reported.[6] In that case, it is believed that oxy-hydroxide species, specifically $HFeO^{2-}$, are formed.[7] These species are soluble in soil and water and, as a result, do not form a protective film on the surface.

Corrosion Behavior of Carbon Steel and Physicochemical Characteristics of the Electrolyte

The electrochemical properties of corroded and scaled iron surfaces as a function of solution composition are not completely understood. However it is recognized that some parameters such as dissolved oxygen (DO), pH, solution flow characteristics, and temperature can influence corrosion rates in pipeline steels.[8,9] Generally, weight loss and corrosion rate as well as corrosion layer increase with increasing pH in the range of 7 to 9. On the contrary, iron corrosion rates decrease at higher pH, consistent with increased corrosion layer.[10–14]On the other hand, the corrosion rate of clean surfaces free of corrosion products generally increases by increasing dissolved oxygen concentration. However the presence of corrosion products can affect oxygen diffusion and retard corrosion.[8,9]Therefore increasing in iron ion content in solution or changes in pH during the experiments, especially for the type of long term tests needed for running weight loss analysis, could affect the corrosion behavior of the sample and difficult the interpretation of the results.[8–14]

The objective of this paper is to investigate the effect of AC on the polarization behavior of carbon steel at different DC biased potentials. This wok compares the results of different electrochemical techniques with weight loss analysis and discusses the correlation between them.

[(1)] National Institute of Science and Technology (NIST), 100 Bureau Drive, Stop 1070, Gaithersburg, MD 20899-1070 USA.

EXPERIMENTAL PROCEDURE

Electrode and Solution

The samples used in this work were fabricated from a pipeline API[(2)] grade X65 (UNS K03014) carbon steel. The chemical composition of X65 was: C 0.04-wt%, Si 0.2-wt%, Mn 1.5-wt%, P 0.011-wt%, S 0.003-wt%, Mo 0.02-wt% and Fe balance. The steel was in the quenched and tempered condition. The steel coupons were manufactured into 15x12x5 mm samples with a threaded hole in one surface for electrical connection. Samples were subsequently ground with SiC papers, starting from120 to 600 grit and cleaned with acetone, ethanol and distilled water, respectively. All tests were performed triplicate to ensure the reproducibility of the results.

A 0.1M NaCl solution was used as electrolyte. The solution volume was 300 mL. The solution was made from analytic grade reagents and 18.2 $M\Omega.cm^2$ deionized water. All tests were conducted at ambient temperature (22 °C) and open to air.

Electrochemical Set-up

Electrochemical measurements were performed using a conventional 3-electrode array. A platinum mesh was used as counter electrode and a saturated calomel electrode (SCE) as reference. In order to prevent cross-contamination, a Luggin capillary was used. Prior to electrochemical measurements, the working electrode was kept in the test solution for 24 hours to ensure a steady state value of corrosion potential.

Potentiostatic Steps.

Potentiostatic tests were conducted in 15 20 mV steps. The duration of each step was 48h. Test started at OCP.

To assess the effect of ferrous/ferric ion content and solution pH on corrosion behavior, three different conditions were examined: i) static solution, ii) intermittent batch replacement of solution (250 mL after each hour) and iii) constant solution replacement at a rate of 8mL/min. Replacement of solution was performed using a peristaltic pump and to insure the cell was mixed, stirring at 60 rpm was also applied. During the test, an aliquot of solution was taken periodically to measure pH and Fe ion content.

An ultraviolet visible spectrophotometer (UVS) was used to determine ferrous (Fe^{2+}) and ferric (Fe^{3+}) ion concentration. The Fe^{3+} content was indirectly obtained by calculating the Fe^{2+} concentration, followed by a separate determination of the Fe_{total} concentration .[15,16]

Potentiostatic Tests.

Potentiostatic tests were performed at potentials of -720, -700, -670, -600, -500, -440, -600 and 0 mV vs. SCE with and without impressed AC potentials. A frequency response analyzer was used to provide the AC signal with AC RMS voltages of 100,200,300,400,500 and 600 mV at a frequency of 60 Hz. The current-time and potential-time of carbon steel under various DC and AC potentials were recorded with the acquisition rate of 0.1 points per seconds.

Weight loss analysis.

Weight loss analysis was conducted in accord with ASTM[(3)] G1.[17] After potentiostatic tests, the

[(2)] American Petroleum Institute (API), 1220 L Street, NW Washington, DC 20005-4070 USA.
[(3)] American Society for Testing and Materials (ASTM), 100 Barr Harbor Drive, PO Box C700, West Conshohocken, PA, 19428-2959 USA.

corrosion product formed on the coupon surface was removed by both mechanical and chemical methods. The mechanical method, including scrubbing, was used to remove loosely adhered corrosion product. To remove tightly bound oxide films, samples were immersed for 25 seconds in Clark solution: concentrated HCl (specific gravity 1.19), 2-wt% Sb_2O_3 and 5-wt% $SnCl_2$.

RESULTS

Effect of Solution Composition on Polarization Behavior

Figure 1 shows the variation of current densities due to changes in the chemical composition of the electrolyte. This figure shows data with and without solution replenishment and stirring. Each solid symbol represents data points obtained from the mean steady state current density value obtained from potentiostatic steps at each DC potential. The solid line represents data taken using the potentiodynamic polarization method (stirred and replenished only).

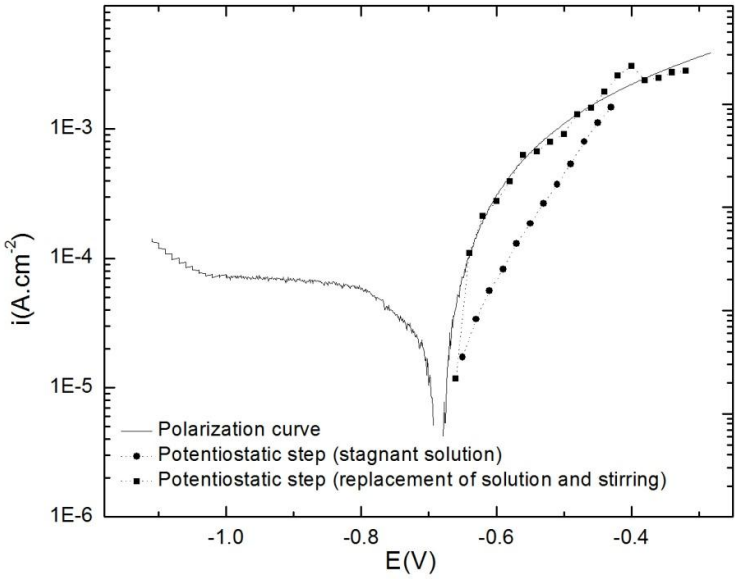

Figure 1: Effect of solution replacement and stirring on current density.

As seen in Figure 1 the current densities obtained from samples in the stagnant solution were consistently lower than those obtain using solution replenishment. Correspondingly, The UVS result showed an increase in Fe^{3+} content with charge passed in stagnant solution at anodic potentials (Figure 2a). In contrast to the stagnant solution, the cell where solution replenishment was used showed constant Fe^{3+} concentration during the test (Figure 2a). On the other hand, results of UVS revealed an increase in Fe^{2+} instead of Fe^{3+} at really high DC potentials and concurrent with an increase in solution pH. Figure 2b shows solution pH with time for high applied anodic potentials (DC=0V vs. SCE). As seen in this figure, an increase in pH in stagnant solution in anodic potentials was observed. In comparison, stirring and solution replacement resulted in relatively constant pH values of approximately pH = 7.0. Therefore, the increase in current density was attributed to the combination of pH and Fe^{3+} that increases corrosion rate vis-à-vis current density.[9,10,14]Hence forth in this paper all data reported here was taken from experiments where stirring and solution replacement was used in order to eliminate any external influences other than imposed AC potential on corrosion behavior of carbon steel.

AC Effect on Corrosion Rate at Different DC Biases

Figure 3 compares corrosion rate with AC (RMS voltage= 600 mV) and without AC as a function of DC potential. Results were obtained by weight loss analysis from potentiostatic tests. Both sets of the data showed the same trend in increasing corrosion rate with increasing DC potential. However the corrosion rate increased in the presence of AC compared to the condition without AC at any given DC bias. The corrosion rate at OCP (-670 mV) with AC was about 10 times higher than that without AC. These findings are consistent with observations made by other authors.[18,19]

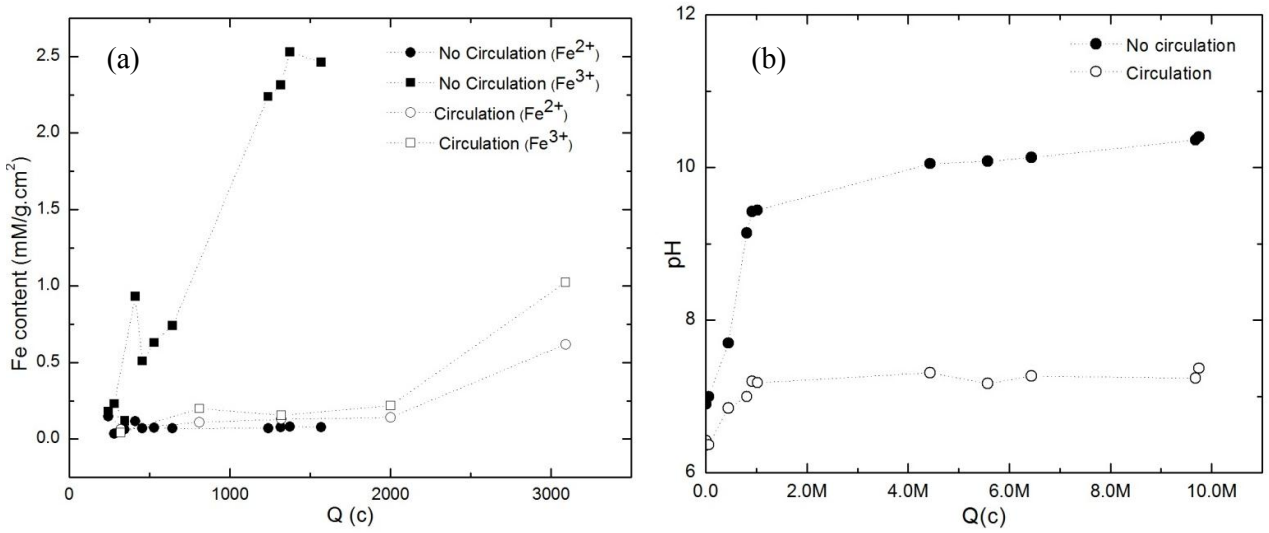

Figure 2: Effect of solution replacement and stirring on: (a) Fe content of electrolyte at DC=-500 mV vs. SCE: (b) pH at DC=0 V vs. SCE.

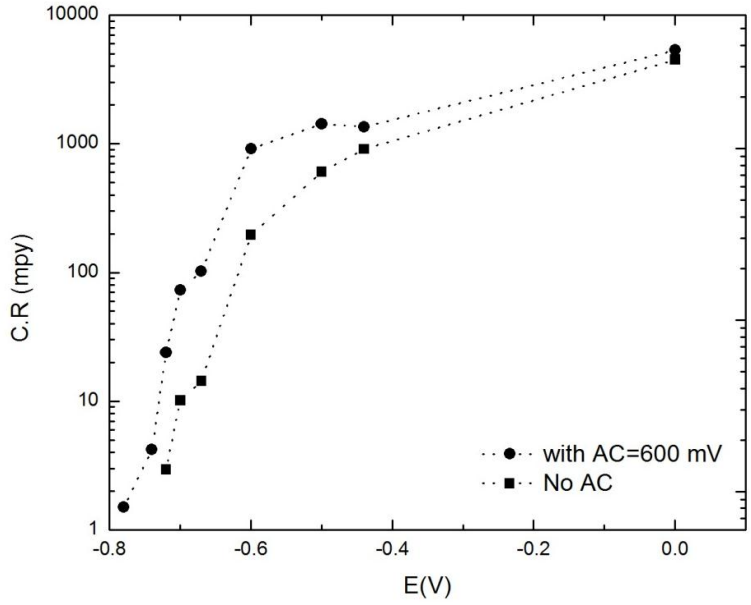

Figure 3: Effect of AC on corrosion rate of carbon steel at different DC biases.

AC Effect on Corrosion Potential and Kinematics Parameters

The values of mass loss obtained at each DC biases (with and without AC), were converted to equivalent current densities using Faraday's law (Equation 1):

$$i = \frac{dw.F}{t.\rho} \quad (1)$$

where: i= current density, dw= mass loss, F= 96485 C.mol^{-1}, t= time, ρ= density of carbon steel (7.8 g.cm^{-3}).

The results along with the potentiodynamic polarization curve without AC (Figure 1) are compared in Figure 4. From this Figure 4it can be seen that with AC there was a shift in corrosion potential (shown by dotted straight line) to lower values. A shift to lower potentials is consistent with the mechanism proposed by Lalvani.[20,21]In that work it was proposed that AC induced corrosion at E_{corr} could be explained by asymmetry in the anodic (β_a) and cathodic (β_c) Tafel slopes. Specifically, it was proposed that an applied AC potential will preferentially increase the rate of the reaction associated with the lower Tafel slope. As it relates to our results, β_a/β_c is equal to 0.42 (from Figure 1 assuming there is no mass transfer by limiting current) consistent with an increase in anodic reaction rate and a decrease in E_{corr} during applied AC potentials. There are also other evidences in support of this model. It can be observed that there is an increase in the corrosion rate or corrosion current density by applying AC and also the Tafel slopes don't change by applying AC.[20–24]These values can be calculated by regression of polarization curve that is also shown in Figure 4. Figure 4 also demonstrates the increasing trend in current densities with AC by increasing of DC biases. The current densities without AC from weight loss/ Faraday's law agreed well with the polarization curve. A more thorough investigation of this mechanism will be presented in future publications.

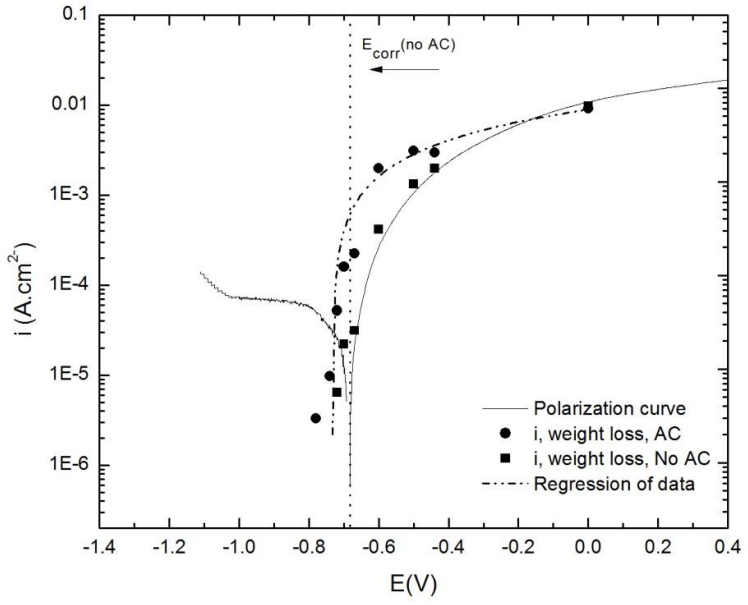

Figure 4: Effect of AC on current density of carbon steel at different DC biases.

To have a better observation on the interactions between AC and DC potentials and their effect on corrosion rate, different AC potentials were also examined (Figure 5). Figure 5 shows the corrosion rate ratio (with AC to without AC) as a function of DC potentials at different AC RMS potential values. There was a decreasing trend in corrosion rate ratios with increasing DC potentials for all AC RMS levels. At lower DC potentials the effect of AC in increasing corrosion rate is more tangible. By lowering the AC RMS potential values, the deviation of corrosion rate from that without AC decreased as well. This reduction of the deviation was more evident at lower potentials. At high DC potentials (0 V vs. SCE) it seemed that the effect of DC potential on corrosion rates predominated over the influence of AC potentials.

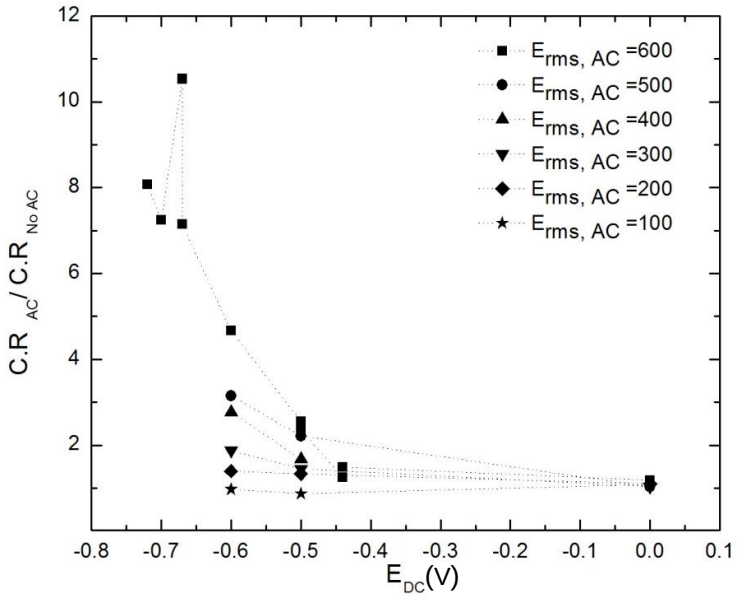

Figure 5: Effect of different AC amplitudes on the ratio of corrosion rate with AC to the corrosion rate without AC at different DC potentials.

Comparison between Electrochemical Techniques and Weight Loss Analysis Method

Figure 6 compares the actual current density from mass loss with that calculated from several different methods identified as positive half-cycle, negative half-cycle and full-cycle. These calculations can be understood using the diagram in Figure 7 which plots a hypothetical AC current response from the sample with time. As the AC current fluctuates between the anodic and cathodic reactions a corresponding positive and negative current is generated: It is assumed that the anodic reaction (positive half-cycle) associated with iron oxidation and the cathodic reaction (negative half cycle) associated with oxygen reduction. Using Faraday's law integral of the each half-cycle relates to the charge passed by the anodic and cathodic reaction.

In this analogy only the positive AC current would result in corrosion as it is the only portion of the curve that contributes to iron oxidation. However, as seen in Figure 6 the calculation of current density from the positive half-cycle grossly over estimates the actual current density of the sample. In addition, the summation of the positive and negative half cycles correlates well with that measured from weight loss. While this phenomenon has been observed before it has not been explained.[25,26]We propose that this phenomena can be explained by generalizing the mechanism proposed by Lalvani for AC corrosion at E_{corr} described above. [20,21]Specifically, for any applied DC potential, if the AC voltage is greater than the overpotential, $E_{peak} > |E_{applied}-E_{corr}|$, a net polarization will result that is proportional to the ratio of the

anodic and cathodic Tafel slopes (β_a and β_c). For example, consider a sample that has an anodic over potential (η_a) of 100 mV and E_{peak} = 200 mV. In the limiting case as β_c goes to infinity, the currents that result from the potentials less than OCP in a cycle go to zero. The result would be a net anodic polarization of the sample. Additional experiments to support this proposal and a formalized model will be presented in future publications.

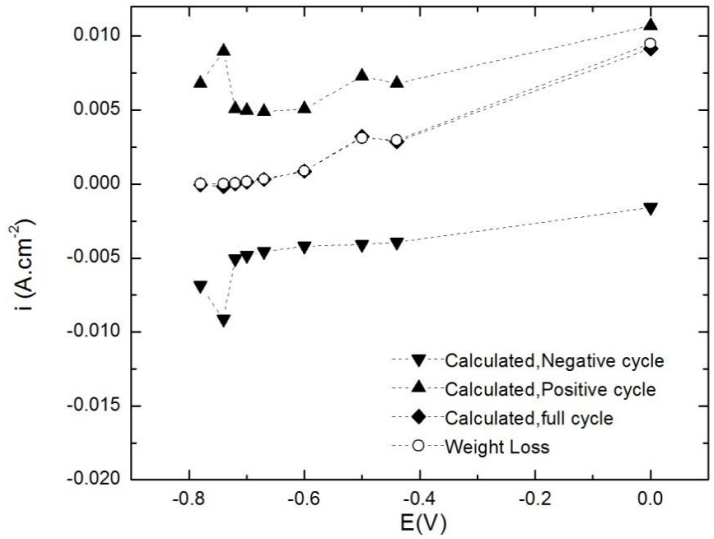

Figure 6: Comparison of corrosion rate with AC from weight loss and three different cycles of potentiostatic test.

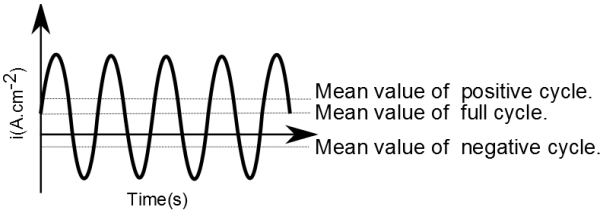

Figure 7: Schematic of sinusoidal AC current density from potentiostatic test.

CONCLUSIONS

In this study it is concluded that replacement of solution made a difference on current density of DC potentiostatic test and therefore the rest of experiments with AC were done with replacement of solution.

It is shown that applied AC currents result in a net DC polarization. It is also indicated that there is a decrease in corrosion potential and an increase in corrosion current density by applying AC. There is no evidence of changing the Tafel slopes by applying AC.

In addition, the average AC current, as measured by the sum of the anodic and cathodic half cycles of the sine wave correlated well with the current density measured by the weight loss analysis and therefore is a good indicator of the corrosion rate.

Finally, different values of DC and AC potentials affect increasing corrosion rate due to AC. It is shown that increasing the AC peak potential increases corrosion rate in the Tafel region but appears to plateau at the same IR limit values at higher potentials as the polarization curve does and the effect of DC potential on corrosion rates predominates. As a result, there is a more pronounced effect of AC near OCP.

ACKNOWLEDGMENTS

The authors wish to acknowledge the financial support of Department of Defense (Grant No. W9132T-11-1-0002). We would especially thank Prof. Nathan Ida and Prof. Joe Payer for their insightful discussions in the study.

REFERENCES

1. McCollum, B., and G.H. Ahlborn, *Am. Inst. Electr. Eng. Trans.* 35 (1916): pp. 301–345.

2. G. Heim ; T. Heim, H.H. ;W. S., *3 R Int.* 32 (1993): p. 246.

3. NACE International Task Group 327, “AC Corrosion State-of-the-Art: Corrosion Rate, Mechanism, and Mitigation Requirements” (2010).

4. SP0177, N.S., *Houston, TX NACE* (2007).

5. Xu, L.Y., X. Su, and Y.F. Cheng, *Corros. Sci.* 66 (2013): pp. 263–268.

6. Hosokawa, Y., F. Kajiyama, and Y. Nakamura, “New CP Criteria for Elimination of the Risks of AC Corrosion and Overprotection on Cathodically Protected Pipelines” (NACE International, 2002).

7. Nielsen, L. V, B. Baumgarten, and P. Cohn, “On-Site Measurements of AC-Induced Corrosion: Effect of AC and DC Parameters,” in CEOCOR Int. Congr. CEOCOR, C/o CIBE, Brussels, Belgium (2004).

8. Sarin, P., V.L. Snoeyink, J. Bebee, W.M. Kriven, and J.A. Clement, *Water Res.* 35 (2001): pp. 2961–2969.

9. Sarin, P., V.L. Snoeyink, J. Bebee, K.K. Jim, M.A. Beckett, W.M. Kriven, and J.A. Clement, *Water Res.* 38 (2004): pp. 1259–1269.

10. McNeill, L.S., and M. Edwards, *J. AWWA* 93 (2001): pp. 88–100.

11. Rice, O., *J. Am. Water Works Assoc.* (1947): pp. 552–560.

12. Stumm, W., *Trans. Am. Soc. Civ. Eng.* 127 (1962): pp. 1–19.

13. Larson, T.E., and R. V Skold, *J. Am. Water Works Assoc.* (1958): pp. 1429–1432.

14. Kashinkunti, R.D., D.H. Metz, D.J. Hartman, and J. DeMarco, “How to Reduce Lead Corrosion without Increasing Iron Release in the Distribution System,” in Proc. 1999 Am. Water Work. Assoc. Water Qual. Technol. Conf. (Tampa Bay FL, 1999).

15. Greenberg, A.E., L.S. Clesceri, and A.D. Eaton, *Washington, DC, USA* (1992).

16. D.K. Nordstrom, C.N.A., *Geochemistry of Acid Mine Waters, Reviews in Economic Geology* (1999).

17. *Stand. A. S. T. M. "G1-03."* (2003): pp. 17–25.

18. Goidanich, S., L. Lazzari, and M. Ormellese, *Corros. Sci.* 52 (2010): pp. 491–497.

19. Jones, D.A., *Corrosion* 34 (1978): pp. 428–433.

20. S. B. Lalvani, X.A.L., *Corros. Sci. 36.6* 36 (1994): pp. 1039–1046.

21. Lalvani, S.B., and X. Lin, *Corros. Sci.* 38 (1996): pp. 1709–1719.

22. Chin, D.-T., and P. Sachdev, *J. Electrochem. Soc.* 130 (1983): pp. 1714–1718.

23. Zhang, R., P.R. Vairavanathan, and S.B. Lalvani, *Corros. Sci.* 50 (2008): pp. 1664–1671.

24. Bosch, R.-W., and W.F. Bogaerts, *Corros. Sci.* 40 (1998): pp. 323–336.

25. Lalvani, S.B., and G. Zhang, *Corros. Sci.* 37 (1995): pp. 1567–1582.

26. Lalvani, S.B., and G. Zhang, *Corros. Sci.* 37 (1995): pp. 1583–1598.